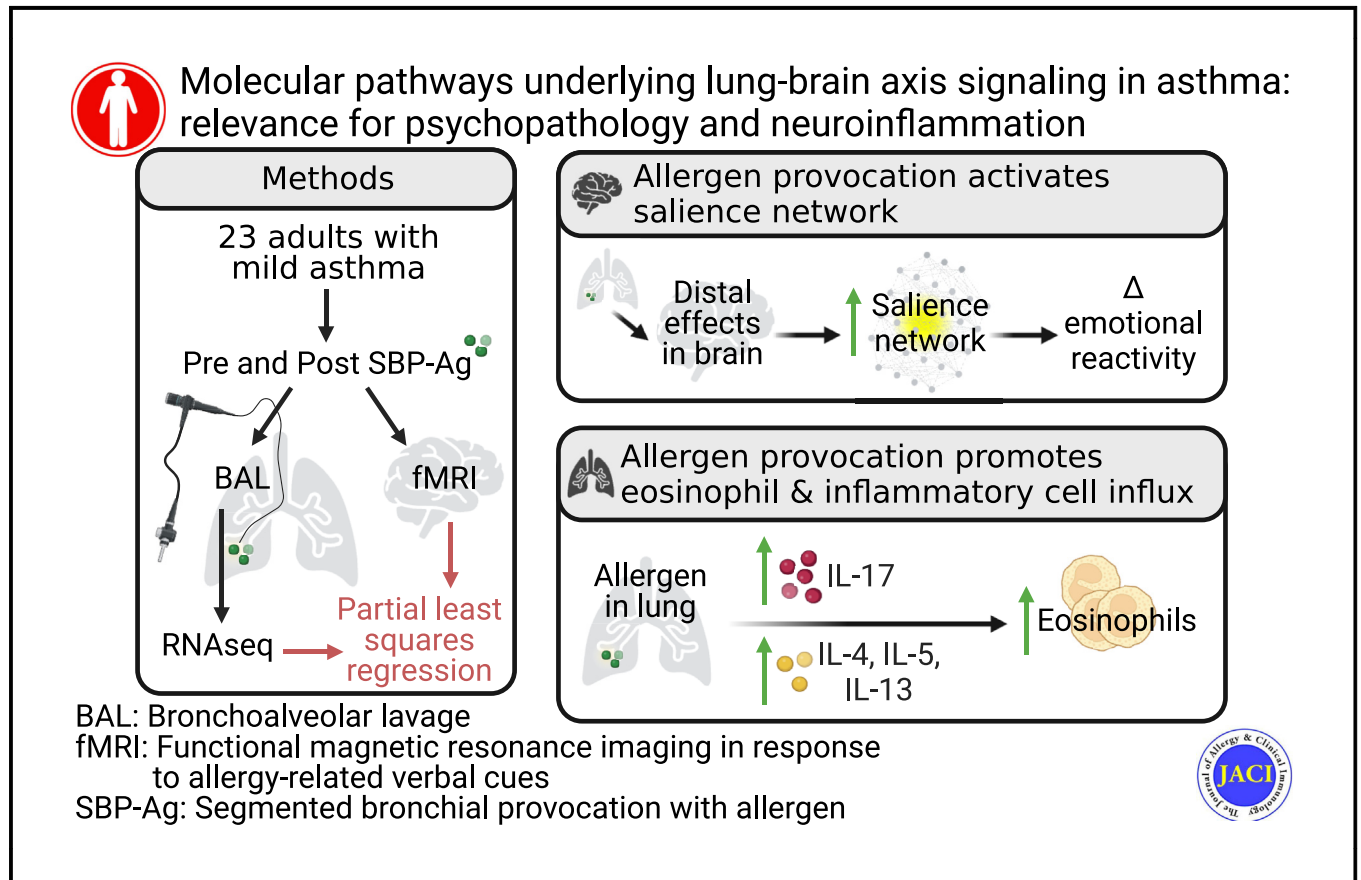


# Molecular pathways underlying lung-brain axis signaling in asthma: Relevance for psychopathology and neuroinflammation



Kimberly A. Dill-McFarland, PhD, Matthew C. Altman, MD, Stephane Esnault, PhD, Nizar N. Jarjour, MD, William W. Busse, MD, Melissa A. Rosenkranz, PhD

## GRAPHICAL ABSTRACT



**Capsule summary:** Systemic effects of airway inflammation on function in the brain’s salience network are related to signaling in T<sub>H</sub>17-related pathways, which may give rise to symptoms of depression and long-term impacts on brain health.

# Molecular pathways underlying lung-brain axis signaling in asthma: Relevance for psychopathology and neuroinflammation



Kimberly A. Dill-McFarland, PhD,<sup>a\*</sup> Matthew C. Altman, MD,<sup>a,b\*</sup> Stephane Esnault, PhD,<sup>c</sup> Nizar N. Jarjour, MD,<sup>c</sup> William W. Busse, MD,<sup>c</sup> and Melissa A. Rosenkranz, PhD<sup>d,e</sup> *Seattle, Wash; and Madison, Wis*

**Background:** Accumulating evidence indicates that asthma has systemic effects and affects brain function. Although airway inflammation is proposed to initiate afferent communications with the brain, the signaling pathways have not been established.

**Objective:** We sought to identify the cellular and molecular pathways involved in afferent lung-brain communication during airway inflammation in asthma.

**Methods:** In 23 adults with mild asthma, segmental bronchial provocation with allergen (SBP-Ag) was used to provoke airway inflammation and retrieve bronchoalveolar lavage fluid for targeted protein analysis and RNA sequencing to determine gene expression profiles. Neural responses to emotional cues in nodes of the salience network were assessed with functional magnetic resonance imaging at baseline and 48 hours after SBP-Ag.

**Results:** Cell deconvolution and gene coexpression network analysis identified 11 cell-associated gene modules that changed in response to SBP-Ag. SBP-Ag increased bronchoalveolar lavage eosinophils and expression of an eosinophil-associated module enriched for genes related to T<sub>H</sub>17-type inflammation (eg, *IL17A*), as well as cell proliferation in lung and brain (eg, *NOTCH1*, *VEGFA*, and *LIF*). Increased expression of genes in this module, as well as several T<sub>H</sub>17-type inflammation-related proteins, was associated with an increase from baseline in salience network reactivity.

**Conclusions:** Our results identify a specific inflammatory pathway linking asthma-related airway inflammation and emotion-related neural function. Systemically, T<sub>H</sub>17-type inflammation has been implicated in both depression and neuroinflammation, with impacts on long-term brain health. Thus, our data emphasize that inflammation in the lung in asthma may have profound effects outside of the lung that may be targetable with novel therapeutic approaches. (*J Allergy Clin Immunol* 2024;153:111-21.)

**Key words:** Asthma, eosinophils, salience network, T<sub>H</sub>17, IL-17, depression, gene expression network analysis, fMRI

Airway inflammation is a cardinal feature of asthma and serves as the primary therapeutic target. However, accumulating

## Abbreviations used

ACQ:	Asthma Control Questionnaire
BAL:	Bronchoalveolar lavage
BDI:	Beck Depression Inventory
BOLD:	Blood oxygen level dependent
CPM:	Count per million
FDR:	False discovery rate
FENO:	Fraction of exhaled nitric oxide
fMRI:	Functional magnetic resonance imaging
ROI:	Regions of interest
SBP-Ag:	Segmental bronchial provocation with allergen
SN:	Salience network
sPLS:	Sparse partial least squares
WLAC:	Whole-lung allergen challenge

evidence suggests that inflammation in asthma extends beyond the airway to result in systemic inflammation,<sup>1</sup> which may give rise to cognitive and affective impairments.<sup>2,3</sup> A long history of both clinical and experimental research has connected asthma with psychological comorbidities, and our previous work sought to uncover the underlying neural mechanisms. In several previous studies, we have demonstrated that allergen provocation of eosinophilic airway inflammation in asthma has an impact on function in the components of the salience network (SN)—the insula, anterior cingulate cortex, and amygdala, in particular. Activity in this brain network shows differential sensitivity to emotional cues during the development of eosinophilic airway inflammation<sup>4,5</sup> and is important in modulating cognitive, affective, and autonomic functions to shift attention toward important information in the body or in the environment,<sup>6,7</sup> in support of homeostatic maintenance.<sup>6</sup> This network has been implicated in the pathophysiology of both depression and dementia,<sup>8,9</sup> which have increased prevalence in asthma,<sup>2,10-13</sup> elevating the clinical importance of efforts to understand how the SN is functionally affected by airway inflammation and to define the signaling pathways involved.

Although our previous work was successful in identifying the key neural components in lung-brain communication in asthma,<sup>4,5,14,15</sup> the molecular pathways engaged during allergic airway inflammation that drive neural modulation remain largely

From <sup>a</sup>the Division of Allergy and Infectious Diseases, University of Washington, Seattle; <sup>b</sup>the Systems Immunology Program, Benaroya Research Institute, Seattle; and <sup>c</sup>the Division of Allergy, Pulmonary and Critical Care Medicine, <sup>d</sup>the Center for Healthy Minds, and <sup>e</sup>the Department of Psychiatry, University of Wisconsin-Madison, Madison.

\*These authors contributed equally to this work.

Received for publication December 13, 2022; revised July 12, 2023; accepted for publication July 20, 2023.

Available online September 19, 2023.

Corresponding author: Melissa A. Rosenkranz, PhD, Center for Healthy Minds, University of Wisconsin-Madison, 625 W. Washington Ave, Madison, WI 53703. E-mail: [melissa.rosenkranz@wisc.edu](mailto:melissa.rosenkranz@wisc.edu).

The CrossMark symbol notifies online readers when updates have been made to the article such as errata or minor corrections

0091-6749/\$36.00

© 2023 American Academy of Allergy, Asthma & Immunology

<https://doi.org/10.1016/j.jaci.2023.07.025>

unknown. On the basis of our previous work, pathways associated with type 2 inflammation were central to our hypotheses. In addition, we hypothesized that T<sub>H</sub>17-associated pathways would be important because IL-17 promotes depression-like behavior in mice<sup>16</sup> and is associated with depression in humans.<sup>17</sup>

To interrogate the relationship between specific molecular changes in the airway provoked by allergen and subsequent changes in SN function, we used bronchoscopy to directly challenge a single segment of the lower airways of patients with asthma. This approach generates an intense airway inflammatory response that is restricted to the challenged segment, resulting in minimal impact on lung function. We used a novel combination of functional magnetic resonance imaging (fMRI) to measure concurrent changes in SN function, coupled with network analysis of bronchoalveolar lavage (BAL) fluid gene and protein expression changes resulting from allergen provocation. By identifying the specific molecular pathways that link communication between the lung and the brain, it is our goal to ultimately identify novel therapeutic targets and potentially prevent the psychological and neurologic consequences associated with the chronic airway inflammation of asthma.

## METHODS

Twenty-three participants with a physician diagnosis of asthma were recruited from Madison, Wis. Participants ranged in age from 19 to 41 years (mean, 26.74 years). All participants had mild asthma and required only bronchodilator medication for asthma management. Participants had allergic sensitization, a positive skin test result for common aeroallergens to be used in provocation procedures, prealbuterol FEV<sub>1</sub> greater than or equal to 70%, and FEV<sub>1</sub> albuterol reversibility greater than or equal to 12% or methacholine provocative concentration causing a 20% fall in FEV<sub>1</sub> less than or equal to 8 mg/mL. Patient characteristics are presented in Table 1. Participants were free of respiratory illnesses for 1 month. Individuals with a history of claustrophobia, ferromagnetic implants, traumatic brain injury, neurologic or seizure disorder, or psychosis were excluded. Those requiring psychotropic medication for depression or anxiety were on a stable dose for 6 weeks before enrollment. The University of Wisconsin-Madison Health Sciences Institutional Review Board (Madison, Wis) approved the study.

Our experimental protocol involved 3 visits to the laboratory. During the first visit, participants provided written informed consent, were screened for inclusion and exclusion criteria, and underwent skin testing and a screening whole-lung allergen challenge (WLAC). During the second visit, fMRI data were acquired at baseline, followed by segmental bronchial provocation with allergen (SBP-Ag). During the third visit, 48 hours after the second visit, the identical fMRI protocol was administered, followed by bronchoscopy without allergen. Measures of lung function and airway inflammation were obtained before and after each bronchoscopy. Data were collected across all seasons between August 2016 and July 2019.

Participants underwent WLAC, as previously described,<sup>18</sup> to determine the allergen provocation dose resulting in a 20% reduction in FEV<sub>1</sub> (AgPD<sub>20</sub>). SBP-Ag was performed using AgPD<sub>20</sub>. A bronchoscopy, typically of the right middle lobe, was performed to retrieve BAL fluid at baseline, followed by SBP-Ag. Bronchoscopy was repeated 48 hours after SBP-Ag to retrieve

BAL samples from the same lobe, at a time associated with a maximal inflammatory response.

Lung function was quantified using spirometry, according to the American Thoracic Society standards<sup>19</sup> and indexed as FEV<sub>1</sub>% predicted. Asthma control was assessed using the 6-item Asthma Control Questionnaire (ACQ-6).<sup>20</sup> Depressive symptoms were measured using the Beck Depression Inventory (BDI).<sup>21</sup> Fraction of exhaled nitric oxide (FENO; NIOX System; Aerocrine, Solna, Sweden) was measured in exhaled breath before and after bronchoscopy, according to the American Thoracic Society guidelines<sup>22</sup> and BAL cell differential was determined in pre- and post-SBP-Ag samples. Protein quantification of 65 cytokines, chemokines, and growth factors in BAL fluids was performed using 2 Multiplex Immunoassay kits (HCP2MAG-62 K and HYCTMAG-60K; Millipore, Temecula, Calif) according to the manufacturer's instructions. A Luminex 100 instrument (Luminex Corp, Austin, Tex) was used to generate quantitative data, and abundance was log<sub>10</sub>-transformed (see Table E1 in this article's Online Repository at [www.jacionline.org](http://www.jacionline.org)).

For RNA-sequencing analyses, BAL cells were stored in buffer RLT (Qiagen, Valencia, Calif) at -80°C before RNA extraction. Total RNA was extracted from BAL cell pellets (N = 22) using RNeasy Mini Kit (Qiagen). RNA quantity and quality were assessed using NanoDrop 2000 (Thermo Fisher Scientific, Waltham, Mass) and RNA electrophoresis (Agilent, Santa Clara, Calif). Sequencing libraries were constructed using SMART-Seq v4 Ultra Low Input RNA Kit (Takara, Kusatsu, Shiga, Japan) and clustered onto a flow cell using a cBOT amplification system with a HiSeq SR v4 Cluster Kit (Illumina, San Diego, Calif). Single-read sequencing was performed on a HiSeq2500 sequencer (Illumina), using a HiSeq SBS v4 Kit to generate 58-base reads. Reads were processed using workflows managed on the Galaxy platform including trimming to a minimum quality score of 30, aligning to the GRCh38 reference genome using STAR (v2.4.2a),<sup>23</sup> and quantifying using HTSeq-count (v0.4.1)<sup>24</sup> with ensembl release 91.<sup>25</sup>

Anatomical and functional MRI images were acquired using a GE MR750 3.0-Tesla high-speed imaging device with a 32-channel head coil (General Electric Medical Systems, Milwaukee, Wis). The key elements of the fMRI methods include sagittal echo planar image slices (44 × 3 mm) covering the whole brain (interslice gap, 0.5 mm; in-plane resolution, 3.5 × 3.5 mm; field of view, 224 mm; repetition time, 2000 ms; echo time, 20 ms; and flip angle, 75°). A high-resolution T1-weighted anatomical scan (3-dimensional T1-weighted inversion recovery fast gradient echo image; inversion time, 450 ms; in-plane resolution, 256 × 256 mm; field of view, 256 mm; and axial slices, 192 × 1.0 mm) was acquired for spatial coregistration of functional data. One participant was removed from analysis because of excessive movement.

During fMRI acquisition, participants performed a modified version of the Stroop task<sup>26</sup> to probe the neural response to emotional stimuli that vary in salience. Participants identified the color of asthma-relevant (As; eg, wheeze), negative (Ng; eg, loneliness), and valence-neutral (Ne; eg, curtains) words using an MRI-compatible response box. The As words were words associated with the experience of asthma, generated by individuals with asthma. The Ng and Ne words were selected from the Affective Norms for English Words data set.<sup>27</sup> Thirty-two words

**TABLE I.** Patient characteristics

Characteristics	Pre-SBP-Ag	Post-SBP-Ag	<i>P</i> value*
Age (y)	26 ± 6.7		
Sex: female (%)	52		
Race (%)			
White	83		
Black	8.7		
Mixed	8.7		
FEV <sub>1</sub> screening WLAC	2.5 ± 0.47		
FEV <sub>1</sub> % predicted (%)	91 ± 11	91 ± 9.7	.99
FENO	46 ± 29	65 ± 40	4.1 × 10 <sup>-5</sup>
BAL cell percentage†			
Eosinophil	0.65 ± 0.69	31 ± 29	1.6 × 10 <sup>-4</sup>
Monocyte	83 ± 9.1	48 ± 29	1.4 × 10 <sup>-5</sup>
Neutrophil	2.1 ± 2.4	8.0 ± 12	.053
Lymphocyte	12 ± 6.9	13 ± 5.3	.47
Epithelial	2.6 ± 2.9	0.17 ± 0.39	3.1 × 10 <sup>-3</sup>

Data are presented as mean ± SD, unless specified otherwise.

\*Paired *t* test.

†Benjamini-Hochberg-corrected *P* value across 5 cell types.

of each category were presented in 1 of 4 colors. A 10-second baseline period flanked each run. In each of 2 runs, 48 stimuli (16 per category) were presented for 2 seconds each, with a pseudorandomized inter-stimulus interval of 4 to 8 seconds.

## Data analysis

To examine the impact of SBP-Ag on lung function and airway inflammation, we used paired *t* tests with Benjamini-Hochberg correction of *P* values to evaluate the change from baseline in FEV<sub>1</sub>% predicted, FENO, and cell differentials. Pre- to post-SBP-Ag changes in ACQ and BDI scores were also tested using paired *t* tests.

Cleaning and analysis of RNA-sequencing data were performed in R (v4.0.2)<sup>28</sup> using tidyverse (v1.3.0).<sup>29,30</sup> RNA-sequencing libraries were filtered for quality at median coefficient of variance coverage of less than 0.65, mapped duplicate reads greater than 0.8, and total sequences greater than 1 million (see Table E2 in this article's Online Repository at [www.jacionline.org](http://www.jacionline.org)). No batch effects were detected in principal-component analysis. Gene counts were normalized for RNA composition using trimmed mean of *M* value normalization, filtered to protein-coding genes with at least 1 count per million (CPM) in at least 10% of libraries, and converted to log<sub>2</sub> CPM with quality weights using voom<sup>31</sup> (Table E1). This resulted in 14,346 genes for analysis in 22 paired pre- and postchallenge samples.

For gene module analysis, all genes were linear-modeled for SBP-Ag and filtered to 6863 genes with a false discovery rate (FDR) of less than 0.3 (see Table E3 in this article's Online Repository at [www.jacionline.org](http://www.jacionline.org)). This subset was then modeled separately against eosinophil or neutrophil percentages. Genes were assigned to cell types at an FDR of less than 0.3 and slope greater than 0, resulting in 2787 eosinophil- and 428 neutrophil-associated genes (Table E3). Cell-associated genes were then grouped into modules using Weighted Gene Coexpression Network Analysis<sup>32</sup> with minimum *R*-squared of 0.8, resulting in 9 eosinophil and 2 neutrophil modules (Table E1). Gene modules were associated with functions using STRING protein-

protein interaction networks<sup>33</sup> and hypergeometric enrichment of Broad MSigDB gene sets.<sup>34</sup>

All fMRI data preprocessing and analyses were completed using FSL<sup>35</sup> v5.0, with the following steps: (1) removal of the first 5 volumes, (2) motion correction using MCFLIRT,<sup>36</sup> (3) brain extraction using BET,<sup>37</sup> and (4) registration of the individual functional and anatomical data using the boundary-based registration approach.<sup>38</sup> A 12-degree of freedom affine transformation, using FLIRT,<sup>36</sup> followed by FNIRT nonlinear transformation, was used to register functional data to standard space (Montreal Neurological Institute 152). Individual participant data for each run were analyzed using a general linear model with separate regressors for each condition (ie, As, Ng, and Ne), formed by convolving a stimulus boxcar function with an ideal hemodynamic response function. The model included motion parameters and their derivatives to adjust for motion-related artifact. The general linear model yielded a set of contrast maps (As-Ne, Ng-Ne, and As-Ng) for each individual. These contrast maps were spatially blurred using a 5-mm full-width-at-half-maximum Gaussian spatial filter.

*A priori* regions of interest (ROI) in the SN were selected on the basis of our previous published work.<sup>4,5,15,39</sup> The insular cortex was a central focus of these analyses, given its prominence as a hub in the SN and its consistent presence in pathways activated by peripheral inflammation.<sup>4,5,40-45</sup> Functional subregions of the insula were defined by Deen et al.<sup>46</sup> We identified an additional insula ROI on the basis of increased regional responsiveness to the Stroop task during airway inflammation.<sup>5</sup> The anterior cingulate cortex was selected on the basis of its involvement in brain-body communication during inflammation, both in our own work and in that of others,<sup>4,40,44,45,47</sup> and subdivisions were defined on the basis of the Harvard-Oxford Atlas. In addition, a perigenual anterior cingulate cortex ROI was defined (dilated 2×) by results described by Rosenkranz et al.<sup>4</sup> Finally, the amygdala, defined anatomically by the Harvard-Oxford Atlas, was selected on the basis of its sensitivity to peripheral inflammation and important role in emotion processing.<sup>15,44,48</sup>

Changes in response to SBP-Ag were calculated as post- minus pre-SBP-Ag values within-participant for gene modules, proteins, and fMRI blood oxygen level dependent (BOLD) percent signal change. Sparse partial least squares (sPLS) regression was used to select gene modules and proteins that most strongly associate with changes in fMRI (mixOmics<sup>49</sup>) in the subset of participants with all data types (N = 14). Models were tuned using axis loadings and mean absolute error. Two axes were chosen because this explained most (66%) of the variation in BOLD response. In total, 14 predictor features were mapped to component 1 and 2 predictor features to component 2. Correlations were calculated using the Pearson method (Table E3). Sequences are available in the National Center for Biotechnology Information Gene Expression Omnibus (GSE182733), and R code can be found at [https://github.com/altman-lab/P337\\_MINA\\_BAL\\_public](https://github.com/altman-lab/P337_MINA_BAL_public). The graphical abstract was created using Biorender.com.

## RESULTS

### Lung function, depression, asthma control, and airway inflammation

FEV<sub>1</sub> and BDI scores showed no significant change from pre- to post-SBP-Ag (*P* > .1). In contrast, ACQ scores increased

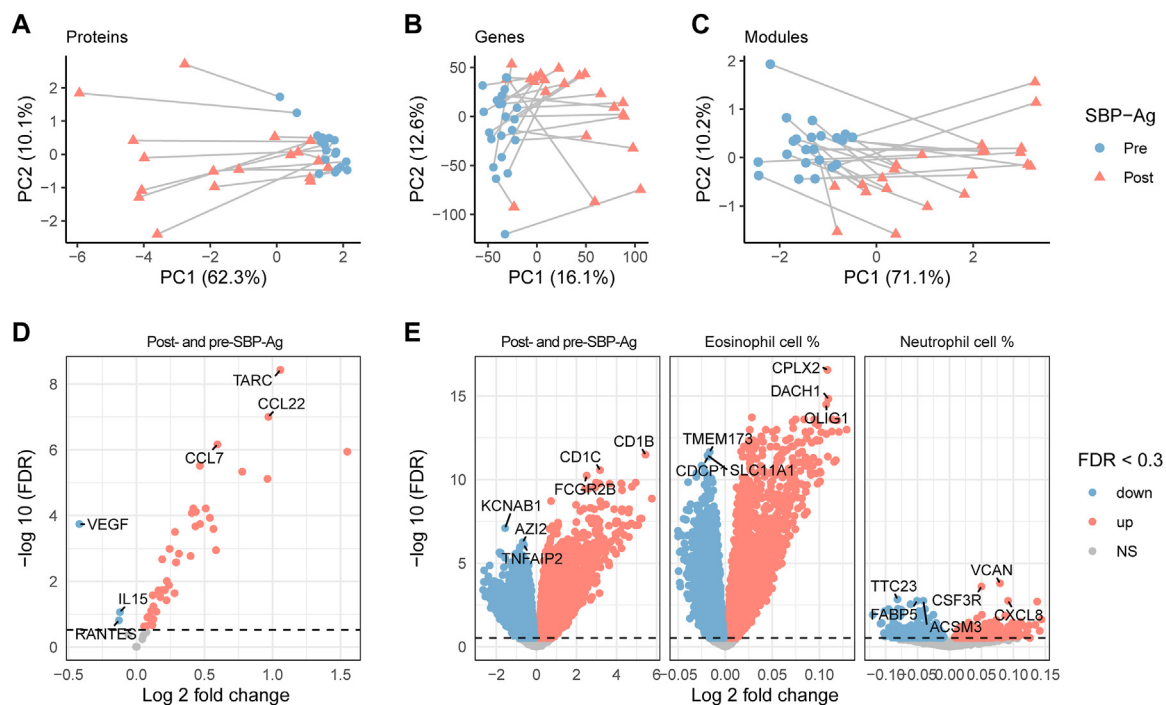


**FIG 1.** Proteins, genes, and gene modules affected by SBP-Ag. **A-C,** Principal-component analysis of 55 cytokine proteins ( $\log_{10}$  pg/mL) (Fig 1, A), 14,346 genes ( $\log_2$  CPM) (Fig 1, B), and 11 eosinophil- and neutrophil-associated gene modules (mean  $\log_2$  CPM) (Fig 1, C). Sample color and shape indicate pre- and post-SBP-Ag with paired samples from the same donor connected by a line. **D and E,** Volcano plots of cytokine proteins pre- and post-SBP-Ag (Fig 1, D) and genes pre- and post-SBP-Ag as well as against eosinophil and neutrophil cell percentages (Fig 1, E). *Orange circles* indicate proteins and genes with significantly higher expression post-SBP-Ag or positively associated with cell percentages (FDR < 0.3). *Blue circles* indicate proteins and genes with significantly lower expression. The top 3 most significant up and down proteins and genes are labeled. *NS*, Not significant.

significantly ( $0.72 \pm 0.61$  to  $0.91 \pm 0.52$ ;  $P = .02$ ), indicating a reduction in asthma control, as did FENO ( $46 \pm 29$  ppb to  $65 \pm 40$  ppb;  $P = 4.1 \times 10^{-5}$ ). Cell differentials revealed that the cellular response to SBP-Ag was dominated by increases in the percentage of eosinophils (from 0.65% to 31.3%; FDR-adjusted  $P = 1.56 \times 10^{-4}$ ) and relative decreases in monocytes (from 83.1% to 47.6%; FDR =  $1.40 \times 10^{-5}$ ) and epithelial cells (from 2.61% to 0.17%; FDR =  $3.12 \times 10^{-3}$ ). Neutrophils (FDR = 0.053) and lymphocytes (FDR = 0.466) were not affected by SBP-Ag (see Fig E1, A, in this article's Online Repository at [www.jacionline.org](http://www.jacionline.org)). Cytokine protein abundance showed global changes (Fig 1, A), with most proteins significantly affected (47 of 55; FDR < 0.3; Fig 1, B; see also Table E4 in this article's Online Repository at [www.jacionline.org](http://www.jacionline.org)). Among these, most SBP-Ag-affected proteins were also positively associated with either eosinophils (44 of 47) and/or neutrophils (43 of 47; FDR < 0.3; Table E4).

### RNA sequencing

From 14,346 post-filter genes, 6,863 showed a change in expression after SBP-Ag (FDR < 0.3; Table E3; Fig 1, C and D). This subset of genes was then compared separately for relationships to eosinophil or neutrophil percentages. Genes were associated with cell types for which they had an FDR of less than 0.3 and a positive slope, resulting in 2,787 eosinophil- and 428 neutrophil-associated genes (Table E3). Next, cell-associated

genes were grouped into modules using Weighted Gene Coexpression Network Analysis.<sup>32</sup> In total, 2,818 SBP-Ag- and cell-associated genes were collapsed into 9 eosinophil- and 2 neutrophil-associated modules. Mean gene expression in modules captured much of the gene-level changes pre- to post-SBP-Ag (Fig 1, E; Table E3).

### fMRI analyses

The neural response to asthma-relevant words relative to valence-neutral words showed wide variability (Fig E1, B). Overall, there was no main effect of challenge on mean BOLD response in any of the ROI examined (FDR > 0.3; see Table E5 in this article's Online Repository at [www.jacionline.org](http://www.jacionline.org)), which is not surprising in a sample of this size. However, in confirmation of our previous work,<sup>4,5</sup> we found the expected positive association between the change in the proportion of BAL eosinophils and BOLD response to asthma cues in the SN, most prominently in the anterior insula ( $R = 0.46$ ;  $P < .05$ ; Fig E1, C).

In sPLS analyses examining key associations between allergen-induced changes in gene and protein expression in the airway with changes in SN activity, component 1 represented significant positive correlations among allergen-induced increases in a gene expression module (EOS02) containing 416 eosinophil-associated genes and 13 proteins (most strongly FLT3LG and IL-17A) with increased activity in SN nodes (Fig 2). This result explained 36.7% of the

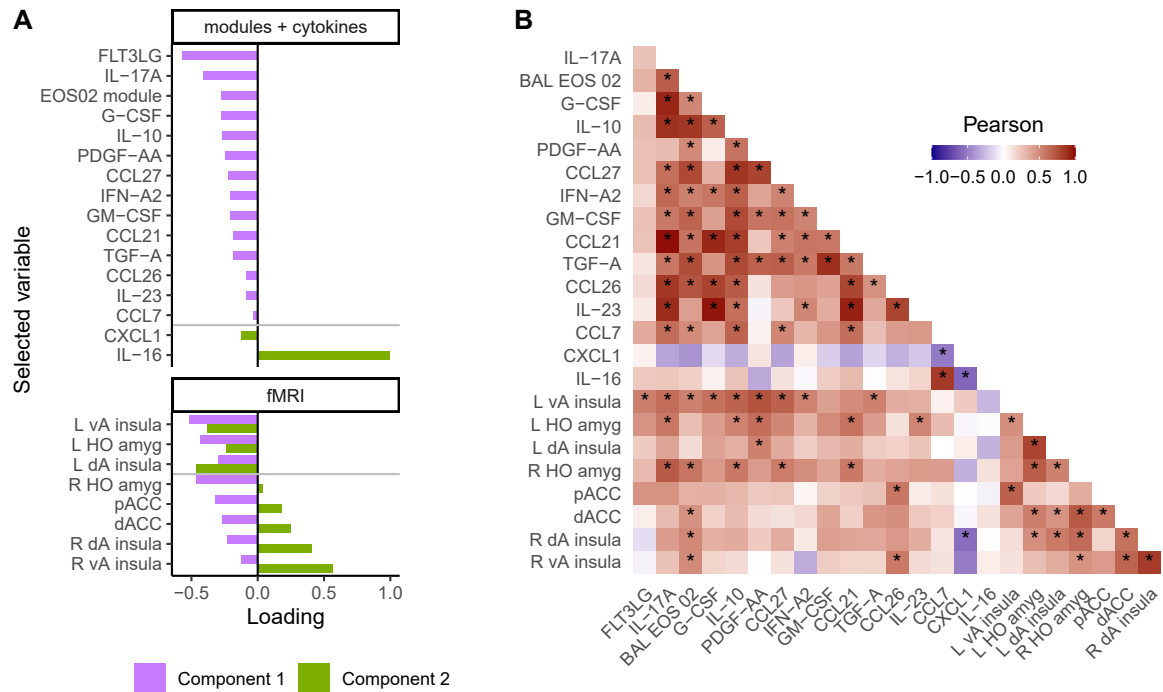


**FIG 2.** sPLS regression of SBP-Ag-induced changes in the lung and brain. Measures were assessed as post-minus pre-SBP-Ag. **A**, Axis loadings for gene modules and cytokine proteins against fMRI outcomes. The first 2 components explain more than 45% of variation in module and cytokine data as well as more than 65% of fMRI. Horizontal gray lines note where component 2 trends change. **B**, Pearson correlation of sPLS-selected variables. Variables are ordered as in Fig 2, A. amyg, Amygdala; dA, dorsal anterior; HO, Harvard-Oxford Atlas-defined; L, left; p/dACC, pregenual/dorsal anterior cingulate cortex; R, right; vA, ventral anterior. \*Pearson  $P < .05$ .

variability in change in gene and protein levels and 45.4% of the variability in change in BOLD response in the SN with a correlation  $R$  value of 0.7. sPLS component 2 represented mixed negative (CXCL1) and positive (IL-16) correlations of change in protein levels with right-sided insula activity specifically (Fig 2). This result explained an additional 11.1% of the variability in change in gene and protein levels and 20.9% of the variability in change in BOLD response with a correlation  $R$  value of 0.9.

In identification of functional gene networks, we focused on component 1 because of its robust and consistent correlations across SN nodes. We found that the SBP-Ag-induced genes and proteins selected by sPLS have known functional interactions as evidenced by a significant interaction network of high confidence interactions in the STRING database<sup>33</sup> ( $P = 1.2 \times 10^{-5}$ ; Fig 3). The most central proteins in this network included mitogen-activated protein kinase 3 (degree = 30; betweenness = 3989), VEGFA (degree = 30; betweenness = 3297), CDK3 (degree = 20; betweenness = 2286), and NOTCH1 (degree = 16; betweenness = 1814). Collectively, this network was functionally enriched for pathways related to cytokine signaling, leukocyte chemotaxis, and tissue growth (Table E3). It includes key components of  $T_H17$  inflammation, including IL-17A, IL-23A, and FLT3LG, a cytokine critical to sustaining expansion of  $T_H17$  cells in the lung,<sup>50</sup> as well as multiple molecules with overlapping roles in neuronal, vascular, and lung cell proliferation (eg, NOTCH1, VEGFA, and LIF).<sup>51-53</sup>

Expression of these genes and proteins increased with SBP-Ag, with the magnitude of change positively relating to both the directionality and the magnitude of changes in SN activity, as exemplified by the relationship between the EOS02 module and IL-17A protein levels and responsiveness of the left ventral anterior insula to asthma-specific cues (Pearson  $R \geq 0.54$ ;  $P < .05$ ; Fig 4). These associations were stronger than those between the SN and eosinophil cell proportions alone (Pearson  $R = 0.46$ ; Fig 4) and stronger than associations with type 2 inflammatory pathways represented by the EOS01 module, mast cell genes, or IL-5 and IL-13 proteins (see Fig E2 in this article's Online Repository at [www.jacionline.org](http://www.jacionline.org)). In addition, although TNFA protein itself increased significantly with SBP-Ag, TNFA abundance was not significantly correlated with changes in the SN, nor was IL-6 and other related genes and proteins selected in sPLS analysis (Fig E2).

## DISCUSSION

The eosinophil-associated pathways reflected in the EOS02 module and associated proteins emerged as the molecular signature of airway inflammation most closely associated with affect-related changes in SN function. These data are consistent with previous work and importantly advance our understanding of the specific biology linking lower airway inflammation with neural changes in patients with asthma but also add an important level of molecular specificity. The genes and proteins functionally

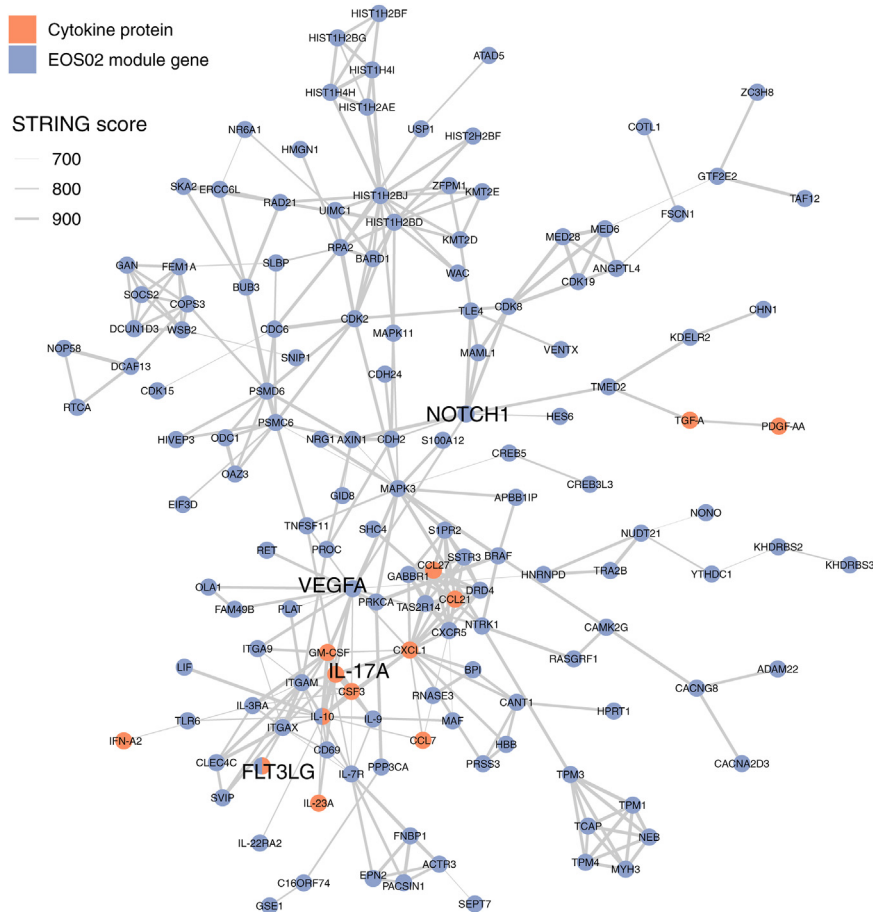


**FIG 3.** STRING network of sPLS-selected genes and proteins associated with neuronal responses to SBP-Ag. Color indicates EOS02 module genes (purple) and protein cytokines (orange) significantly associated with 1 or more fMRI outcome. Edges with STRING combined score greater than 700 are shown in gray with width corresponding to score. The largest cluster of 147 nodes is shown. A small cluster (N = 49) and isolated nodes (N = 196) are not shown.

central to this module were linked more to a  $T_H17$  response with mixed inflammatory and proliferative pathways rather than to the canonical type 2 inflammatory pathways typically associated with eosinophils and asthma.<sup>54</sup> Indeed, type 2 pathways (ie, EOS01 module and IL-4, IL-5, and IL-13 proteins) were not strongly associated with increased activation in the SN (Table E3) in the present study. We similarly did not detect significant associations with other aspects of asthma-related inflammation, including mast cell genes or IL-6 signaling, although these also increased following SBP-Ag. The absence of a mast cell signal may relate to the timing of sample collection at 48 hours postchallenge.<sup>55</sup>  $T_H17$  inflammation has been variably associated with eosinophilic or neutrophilic asthma<sup>56,57</sup> and can be coincident with type 2 inflammation.<sup>58-60</sup> In a previous work,<sup>61</sup> we showed that eosinophils spontaneously release IL-1 $\beta$  to increase the production of IL-17A by activated memory CD4<sup>+</sup> T cells, which is consistent with our current data showing that the IL-17A signal is closely linked with an eosinophilic response rather than with neutrophils. The baseline percentage of  $T_H17$  cells in circulation has been shown to be elevated, even in mild asthma, and to increase, together with IL-17 expression, following allergen challenge.<sup>62</sup> Interestingly, during stress<sup>16</sup> or episodes of inflammation,<sup>63,64</sup>  $T_H17$  cells can accumulate in the brain. This

is noteworthy because systemic administration of IL-17 in animal models evokes depressive-like behavior<sup>65</sup> and anti-IL-17 confers resistance.<sup>16</sup> Consistent with its effect in animal models, IL-17 expression is elevated in depression in humans<sup>66,67</sup> and is associated with depression that is treatment-resistant. Taken together, our results provide a potential direct link between asthma and depression through  $T_H17$  rather than through canonical type 2 inflammation.

In concert with the SBP-Ag–induced upregulation of genes in the  $T_H17$  inflammatory pathway, *NOTCH1* and *VEGFA* were central to the STRING network of proteins and genes in the EOS02 module that was correlated with SN responses to allergen (Fig 2). These genes and their associated pathways have important implications for both asthma and neuronal function. In asthma, *NOTCH1* is involved in multiple aspects of pathophysiology,<sup>68</sup> drives differentiation of  $T_H17$  cells,<sup>69,70</sup> and is essential for eosinophil chemotaxis and transendothelial migration.<sup>71</sup> *VEGFA* plays an important role in airway blood vessel growth in asthma and induces vascular permeability and leakage, in addition to its participation in allergic sensitization and type 2 inflammation.<sup>72</sup> In the brain, IL-17 activates *NOTCH1*,<sup>73</sup> which regulates differentiation of neural stem cells<sup>52,74</sup> and promotes neuroinflammation during neural injury or neurodegeneration via regulation of astrocyte

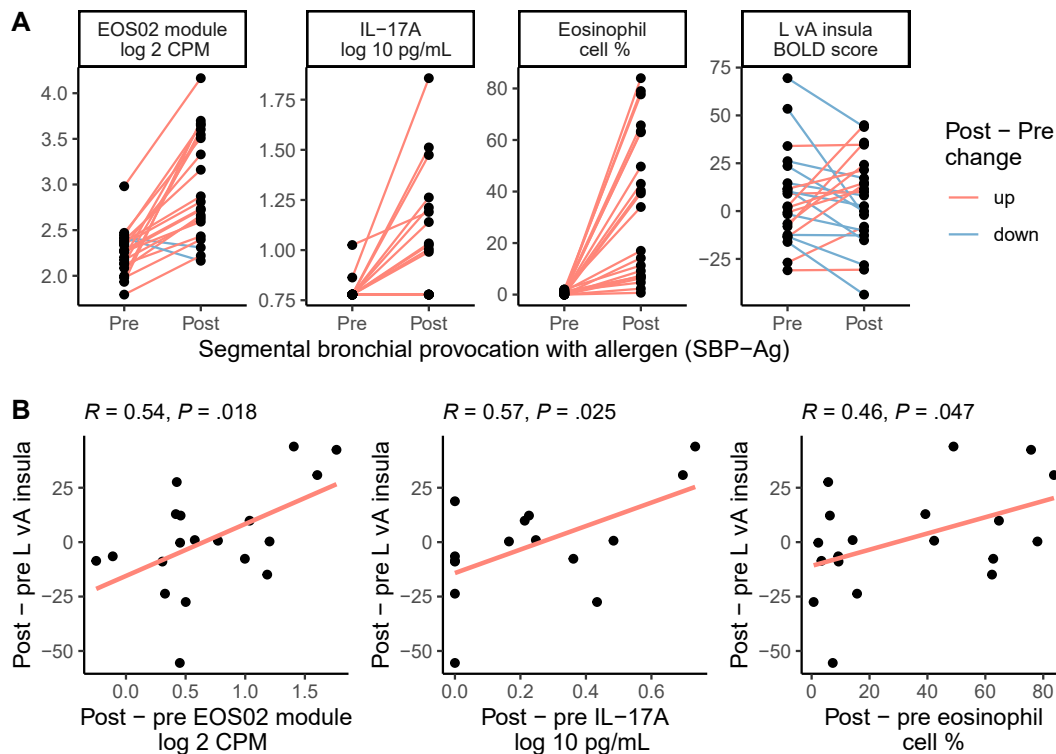


**FIG 4.** EOS02 module genes and IL-17A protein associated with L Va insula response to SBP-Ag. **A**, Eosinophil cell percentage, mean log<sub>2</sub> CPM expression of EOS02 module genes, log<sub>10</sub> pg/mL abundance of IL-17A protein, and L vA insula pre- and postsegmental bronchial provocation with allergen (SBP-Ag). Paired samples from the same individual are connected by a line colored by post- pre changes up (red) or down (blue). **B**, Pearson correlation (*R*) of L vA insula with eosinophil percentage, EOS02 module, and IL-17A protein. Trend lines represent a best fit linear model. L vA, left ventral anterior.

differentiation and proliferation and microglial activation.<sup>52</sup> VEGFA is integrally involved in angiogenesis in the brain. It is also produced by reactive astrocytes, leading to increased blood-brain barrier permeability and degradation of barrier function, which is a major contributor to neuroinflammation,<sup>75</sup> an important factor in stress-related vulnerability versus resilience to depression.<sup>76</sup> Thus, the implication of NOTCH1 and VEGFA in the relationship between SBP-Ag-induced airway changes and neural function suggests that airway inflammation may influence neuronal activity, at least in part, via neuroinflammatory pathways, contributing to negative emotional and cognitive outcomes. Indeed, NOTCH1 has previously been implicated in vulnerability to psychopathology.<sup>77</sup>

Collectively, our data support previous observations that allergen-driven eosinophilic inflammation is associated with enhanced reactivity in brain networks important in regulating emotion.<sup>4,5</sup> Here, we further provide a proposed mechanism of action wherein T<sub>H</sub>17 inflammation, linked to expression of neuronal and vascular signaling molecules in the lung, promotes neuroinflammation, and ultimately emotional and cognitive dysfunction. There are multiple potential ways through which changes in gene and protein expression in the lung could influence neuronal function, resulting in the pattern of associations reported here. It is possible that T<sub>H</sub>17 cells in the lung migrate to the brain, where they promote

neuroinflammation through astrocyte and microglial differentiation and activation. Glia are also intimately involved in regulating neurotransmission and neuronal activity by shaping synaptic architecture and function<sup>78</sup> and through regulating the amount of glutamate in the synapse.<sup>79</sup> This mechanistic hypothesis is supported by recent work in which we found that the concentration of a blood-based marker of reactive astrocytes in asthma was highly related to changes in brain microstructure, indicating the presence of neuroinflammation.<sup>80</sup> Our hypothesis is further supported by a rodent model of mixed T<sub>H</sub>17 and type 2 asthma, wherein allergen exposure selectively increased the number of T<sub>H</sub>17 cells in the brain. This increase was associated with morphologically activated microglia in the subformal organ, which projects to the SN, as well as changes in neuronal activity in SN nodes.<sup>81</sup>

It is important to note that this study was limited to measuring changes in gene expression in BAL fluid cells and not directly in brain cells. However, there is evidence that differential expression of genes in peripheral immune cells is mirrored in neurons and brain immune cells.<sup>82</sup> For example, genes differentially expressed in lymphocytes from patients with schizophrenia were found to have concordant differential expression in postmortem brain samples (both neurons and immune cells).<sup>83</sup> Furthermore, the evaluation of gene expression changes, including NOTCH1 and VEGFA, in cells drawn from peripheral samples shows

neuropathophysiological predictive value and is being explored as a noninvasive approach in determining the clinical trajectory of cognitive decline.<sup>84</sup> Nonetheless, this is a known limitation of the present study and will require confirmation in an animal model. A further limitation of the study was the absence of a control or placebo challenge. In a previous work,<sup>4</sup> we compared the neural response to WLAC to that of inhaled saline, which revealed no significant changes, obviating the need to understand immune signaling pathways underlying this effect in the present study. Finally, given the relative homogeneity of our sample (83% non-Hispanic White), our results may not generalize to a more diverse sample and should be validated in a larger, more representative sample.

Our results identify the importance of T<sub>H</sub>17 inflammation and associated NOTCH1 and VEGFA signaling in the interaction between airway inflammation and emotion-related SN activity. More broadly, our data emphasize that asthma-related inflammation has a systemic component with potentially profound effects outside the lung. The connection of T<sub>H</sub>17 activity with expression of genes important in neuroinflammation raises new hypotheses regarding the scope of the impact of airway inflammation on the brain. We speculate that targeted control of specific aspects of airway inflammation in asthma is an important step to prevent or reduce comorbid conditions including depression and cognitive dysfunction as well as deterioration in brain health more generally.

## DISCLOSURE STATEMENT

This work was supported by the National Heart, Lung, and Blood Institute (grant no. R01HL123284 to W.W.B.).

Disclosure of potential conflict of interest: M. C. Altman reports personal fees from Sanofi-Regeneron, outside the submitted work. W. W. Busse reports consulting fees/honoraria from GlaxoSmithKline, Novartis, AstraZeneca, Regeneron, Sanofi, and Genentech; and royalties from Elsevier. N. N. Jarjour received research funding from AstraZeneca for extension of the National Institutes of Health-funded severe asthma research program; and received consulting fees over the past 3 years (<\$5000) from GlaxoSmithKline with regard to severe asthma treatment. The rest of the authors declare that they have no relevant conflicts of interest.

We acknowledge the contributions of Corrina Frye, Danika Klaus, Amy Dresen, Loren Denlinger, Richard Cornwell, Nathan Sandbo, Gina Crisafi, Tina Palas, Jeni Nestler, Hailey Imhoff, Jenelle Grogan, Evelyn Falibene, Michele Wolff, Lori Wollet, Julia Bach, Paige Lowell, Angela Schraml, Renee Szakaly, Ashlee Lindsay, Heather Floerke, and Andrew Maddox in the collection and analysis of data presented here. We also thank the research participants from whom these data were acquired for their contributions to this work.

### Key messages

- Airway inflammation has an impact on how the brain responds to emotional information.
- Changes in T<sub>H</sub>17-related inflammation are associated with brain impacts of asthma.
- T<sub>H</sub>17 signaling pathways may contribute to psychological and neurologic sequelae of asthma.

## REFERENCES

1. Tattersall MC, Evans MD, Korcarz CE, Mitchell C, Anderson E, DaSilva DF, et al. Asthma is associated with carotid arterial injury in children: the Childhood Origins of Asthma (COAST) cohort. *PLoS One* 2018;13:1-12.
2. Trojan TD, Khan DA, Defina LF, Akpotaire O, Goodwin RD, Brown ES. Asthma and depression: the Cooper Center Longitudinal Study. *Ann Allergy Asthma Immunol* 2014;112:432-6.
3. Irani F, Barbone JM, Beausoleil J, Gerald L. Is asthma associated with cognitive impairments? A meta-analytic review. *J Clin Exp Neuropsychol* 2017;39:965-78.
4. Rosenkranz MA, Busse WW, Johnstone T, Swenson CA, Crisafi GM, Jackson MM, et al. Neural circuitry underlying the interaction between emotion and asthma symptom exacerbation. *Proc Natl Acad Sci U S A* 2005;102:13319-24.
5. Rosenkranz MA, Busse WW, Sheridan JF, Crisafi GM, Davidson RJ. Are there neurophenotypes for asthma? Functional brain imaging of the interaction between emotion and inflammation in asthma. *PLoS One* 2012;7:e40921.
6. Seeley WW. The salience network: a neural system for perceiving and responding to homeostatic demands. *J Neurosci* 2019;39:9878-82.
7. Menon V, D'Esposito M. The role of PFC networks in cognitive control and executive function. *Neuropsychopharmacology* 2022;47:90-103.
8. Pasquini L, Nana AL, Toller G, Brown JA, Deng J, Staffaroni A, et al. Salience network atrophy links neuron type-specific pathology to loss of empathy in frontotemporal dementia. *Cereb Cortex* 2020;30:5387-99.
9. McTeague LM, Rosenberg BM, Lopez JW, Carreon DM, Huemer J, Jiang Y, et al. Identification of common neural circuit disruptions in emotional processing across psychiatric disorders. *Am J Psychiatry* 2020;177:411-21.
10. Rusanen M, Ngandu T, Laatikainen T, Tuomilehto J, Soininen H, Kivipelto M. Chronic obstructive pulmonary disease and asthma and the risk of mild cognitive impairment and dementia: a population based CAIDE study. *Curr Alzheimer Res* 2013;10:549-55.
11. Peng Y-H, Wu B-R, Su C-H, Liao W-C, Muo C-H, Hsia T-C, et al. Adult asthma increases dementia risk: a nationwide cohort study. *J Epidemiol Community Health* 2015;69:123-8.
12. Chen M-H, Li C-T, Tsai C-F, Lin W-C, Chang W-H, Chen T-J, et al. Risk of dementia among patients with asthma: a nationwide longitudinal study. *J Am Med Dir Assoc* 2014;15:763-7.
13. Goodwin RD, Scheckner B, Pena L, Feldman JM, Taha F, Lipsitz JD. A 10-year prospective study of respiratory disease and depression and anxiety in adulthood. *Ann Allergy Asthma Immunol* 2014;113:565-70.
14. Rosenkranz MA, Esnault S, Christian BT, Crisafi G, Gresham LK, Higgins AT, et al. Mind-body interactions in the regulation of airway inflammation in asthma: a PET study of acute and chronic stress. *Brain Behav Immun* 2016;58:18-30.
15. Rosenkranz MA, Esnault S, Gresham L, Davidson RJ, Christian BT, Jarjour NN, et al. Role of amygdala in stress-induced upregulation of airway IL-1 signaling in asthma. *Biol Psychol* 2022;167:108226.
16. Beurel E, Harrington LE, Jope RS. Inflammatory T helper 17 cells promote depression-like behavior in mice. *Biol Psychiatry* 2013;73:622-30.
17. Beurel E, Lowell JA. Th17 cells in depression. *Brain Behav Immun* 2018;69:28-34.
18. Kelly EA, Esnault S, Liu LY, Evans MD, Johansson MW, Mathur S, et al. Mepolizumab attenuates airway eosinophil numbers, but not their functional phenotype, in asthma. *Am J Respir Crit Care Med* 2017;196:1385-95.
19. Anonymous. Standardization of spirometry. *Am J Respir Crit Care Med* 1995;152:1107-36.
20. Juniper EF, Buist AS, Cox FM, Ferrie PJ, King DR. Validation of a standardized version of the Asthma Quality of Life Questionnaire. *Chest* 1999;115:1265-70.
21. Beck AT, Ward CH. An inventory for measuring depression. *Arch Gen Psychiatry* 1961;4:561-71.
22. Silkoff PE, Carlson M, Bourke T, Katial R, Ogren E, Szefer SJ. The AeroCrine exhaled nitric oxide monitoring system NIOX is cleared by the US Food and Drug Administration for monitoring therapy in asthma. *J Allergy Clin Immunol* 2004;114:1241-56.
23. Dobin A, Davis CA, Schlesinger F, Drenkow J, Zaleski C, Jha S, et al. STAR: ultrafast universal RNA-seq aligner. *Bioinformatics* 2013;29:15-21.
24. Anders S, Pyl PT, Huber W. HTSeq—a Python framework to work with high-throughput sequencing data. *Bioinformatics* 2015;31:166-9.
25. Martin FJ, Amode MR, Aneja A, Austine-Orimoloye O, Azov AG, et al. Ensembl 2023. *Nucleic Acids Res* 2023;51:D933-41.
26. Stroop JR. Studies of interference in serial verbal reactions. *J Exp Psychol* 1935;18:643-62.
27. Bradley MM, Lang PJ. Affective Norms for English Words (ANEW): instruction manual and affective ratings. Technical Report C-1, The Center for Research in Psychophysiology, University of Florida; 1999.

28. R Core Team. R: A language and environment for statistical computing. R Foundation for Statistical Computing, Vienna, Austria. 2021. Available at: <https://www.R-project.org/>.
29. Wickham H, Averick M, Bryan J, Chang W, McGowan L, François R, et al. Welcome to the tidyverse. *J Open Source Softw* 2019;4:1686.
30. R Core Team. R: a language and environment for statistical computing. Vienna, Austria: R Foundation for Statistical Computing; 2021.
31. Law CW, Chen Y, Shi W, Smyth GK. voom: Precision weights unlock linear model analysis tools for RNA-seq read counts. *Genome Biol* 2014;15:R29.
32. Langfelder P, Horvath S. WGCNA: an R package for weighted correlation network analysis. *BMC Bioinformatics* 2008;9:559.
33. Szklarczyk D, Gable AL, Lyon D, Junge A, Wyder S, Huerta-Cepas J, et al. STRING v11: protein-protein association networks with increased coverage, supporting functional discovery in genome-wide experimental datasets. *Nucleic Acids Res* 2019;47:D607-13.
34. Mootha VK, Lindgren CM, Eriksson K-F, Subramanian A, Sihag S, Lehar J, et al. PGC-1 $\alpha$ -responsive genes involved in oxidative phosphorylation are coordinately downregulated in human diabetes. *Nat Genet* 2003;34:267-73.
35. Jenkinson M, Beckmann CF, Behrens TEJ, Woolrich MW, Smith SM. FSL. *Neuroimage* 2012;62:782-90.
36. Jenkinson M, Bannister P, Brady M, Smith S. Improved optimization for the robust and accurate linear registration and motion correction of brain images. *Neuroimage* 2002;17:825-41.
37. Smith SM, Jenkinson M, Woolrich MW, Beckmann CF, Behrens TEJ, Johansen-Berg H, et al. Advances in functional and structural MR image analysis and implementation as FSL. *Neuroimage* 2004;23:S208-19.
38. Greve DN, Fischl B. Accurate and robust brain image alignment using boundary-based registration. *Neuroimage* 2009;48:63-72.
39. Rosenkranz MA, Esnault S, Christian BT, Crisafi G, Gresham LK, Higgins AT, et al. Corrigendum to "Mind-body interactions in the regulation of airway inflammation in asthma: a PET study of acute and chronic stress" [*Brain Behav Immun* 2016;58:18-30]. *Brain Behav Immun* 2018;67:398-401.
40. Lekander M, Karshikoff B, Johansson E, Soop A, Fransson P, Lundström JN, et al. Intrinsic functional connectivity of insular cortex and symptoms of sickness during acute experimental inflammation. *Brain Behav Immun* 2016;56:34-41.
41. Karshikoff B, Jensen KB, Ingvar M, Kosek E, Kalpouzos G, Soop A, et al. LPS increases pain sensitivity by decreased pain inhibition and increased insular activation. *Brain Behav Immun* 2015;49:e1.
42. Hannestad J, Subramanyam K, DellaGioia N, Planeta-Wilson B, Weinzimmer D, Pittman B, et al. Glucose metabolism in the insula and cingulate is affected by systemic inflammation in humans. *J Nucl Med* 2012;53:601-7.
43. Harrison NA, Cooper E, Dowell NG, Keramida G, Voon V, Critchley HD, et al. Quantitative magnetization transfer imaging as a biomarker for effects of systemic inflammation on the brain. *Biol Psychiatry* 2015;78:49-57.
44. Felger JC. Imaging the role of inflammation in mood and anxiety-related disorders. *Curr Neuropharmacol* 2017;15:533-58.
45. Eisenberger NI, Inagaki TK, Rameson LT. An fMRI study of cytokine-induced depressed mood and social pain: the role of sex differences. *Neuroimage* 2009;47:881-90.
46. Deen B, Pitskel NB, Pelphrey KA. Three systems of insular functional connectivity identified with cluster analysis. *Cereb Cortex* 2011;21:1498-506.
47. Harrison NA, Brydon L, Walker C, Gray MA, Steptoe A, Critchley HD. Inflammation causes mood changes through alterations in subgenual cingulate activity and mesolimbic connectivity. *Biol Psychiatry* 2009;66:407-14.
48. Phelps EA, LeDoux JE. Contributions of the amygdala to emotion processing: from animal models to human behavior. *Neuron* 2005;48:175-87.
49. Rohart F, Gautier B, Singh A, Cao K-AL. mixOmics: an R package for 'omics feature selection and multiple data integration. *PLoS Comput Biol* 2017;13:e1005752.
50. Shalaby KH, Lyons-Cohen MR, Whitehead GS, Thomas SY, Prinz I, Nakano H, et al. Pathogenic TH17 inflammation is sustained in the lungs by conventional dendritic cells and Toll-like receptor 4 signaling. *J Allergy Clin Immunol* 2018;142:1229-42.e6.
51. Breen EC. VEGF in biological control. *J Cell Biochem* 2007;102:1358-67.
52. Ables JL, Breunig JJ, Eisch AJ, Rakic P. Not(ch) just development: Notch signaling in the adult brain. *Nat Rev Neurosci* 2011;12:269-83.
53. Mathieu ME, Saucourt C, Moumets V, Gauthereau X, Thézé N, Praloran V, et al. LIF-dependent signaling: new pieces in the Lego. *Stem Cell Rev Rep* 2012;8:1-15.
54. Fahy JV. Type 2 inflammation in asthma—present in most, absent in many. *Nat Rev Immunol* 2015;15:57-65.
55. Peters MC, McGrath KW, Hawkins GA, Hastie AT, Levy BD, Israel E, et al. Plasma interleukin-6 concentrations, metabolic dysfunction, and asthma severity: a cross-sectional analysis of two cohorts. *Lancet Respir Med* 2016;4:574-84.
56. Bullens DM, Truyen E, Coteur L, Dilissen E, Hellings PW, Dupont LJ, et al. IL-17 mRNA in sputum of asthmatic patients: linking T cell driven inflammation and granulocytic influx? *Respir Res* 2006;7:135.
57. Doe C, Bafadhel M, Siddiqui S, Desai D, Mistry V, Rugman P, et al. Expression of the T helper 17-associated cytokines IL-17A and IL-17F in asthma and COPD. *Chest* 2010;138:1140-7.
58. Lambrecht BN, Hammad H, Fahy JV. The cytokines of asthma. *Immunity* 2019;50:975-91.
59. Irvin C, Zafar I, Good J, Rollins D, Christianson C, Gorska MM, et al. Increased frequency of dual-positive TH2/TH17 cells in bronchoalveolar lavage fluid characterizes a population of patients with severe asthma. *J Allergy Clin Immunol* 2014;134:1175-86.e7.
60. Christenson SA, van den Berge M, Faiz A, Inkamp K, Bhakta N, Bonser LR, et al. An airway epithelial IL-17A response signature identifies a steroid-unresponsive COPD patient subgroup. *J Clin Invest* 2019;129:169-81.
61. Esnault S, Kelly EAB, Nettenstrom LM, Cook EB, Serooogy CM, Jarjour NN. Human eosinophils release IL-1 $\beta$  and increase expression of IL-17A in activated CD4+ T lymphocytes. *Clin Exp Allergy* 2012;42:1756-64.
62. Naji N, Smith SG, Gauvreau GM, O'Byrne PM. T helper 17 cells and related cytokines after allergen inhalation challenge in allergic asthmatics. *Int Arch Allergy Immunol* 2014;165:27-34.
63. Moynes DM, Vanner SJ, Lomax AE. Participation of interleukin 17A in neuroimmune interactions. *Brain Behav Immun* 2014;41:1-9.
64. Cipollini V, Anrather J, Orzi F, Iadecola C. Th17 and cognitive impairment: possible mechanisms of action. *Front Neuroanat* 2019;13:95.
65. Nadeem A, Ahmad SF, Al-Harbi NO, Fardan AS, El-Sherbeeny AM, Ibrahim KE, et al. IL-17A causes depression-like symptoms via NF $\kappa$ B and p38MAPK signaling pathways in mice: implications for psoriasis associated depression. *Cytokine* 2017;97:14-24.
66. Chen Y, Jiang T, Chen P, Ouyang J, Xu G, Zeng Z, et al. Emerging tendency towards autoimmune process in major depressive patients: a novel insight from Th17 cells. *Psychiatry Res* 2011;188:224-30.
67. Davami MH, Baharlou R, Vasmehjani AA, Ghanizadeh A, Keshtkar M, Dezhkam I, et al. Elevated IL-17 and TGF- $\beta$  serum levels: a positive correlation between T-helper 17 cell-related pro-inflammatory responses with major depressive disorder. *Basic Clin Neurosci* 2016;7:137-42.
68. Huang M-T, Chiu C-J, Chiang B-L. Multi-faceted notch in allergic airway inflammation. *Int J Mol Sci* 2019;20:3508.
69. Li C, Sheng A, Jia X, Zeng Z, Zhang X, Zhao W, et al. Th17/Treg dysregulation in allergic asthmatic children is associated with elevated notch expression. *J Asthma* 2018;55:1-7.
70. Keerthivasan S, Suleiman R, Lawlor R, Roderick J, Bates T, Minter L, et al. Notch signaling regulates mouse and human Th17 differentiation. *J Immunol* 2011;187:692-701.
71. Liu L, Wang H, Xenakis JJ, Spencer LA. Notch signaling mediates granulocyte-macrophage colony-stimulating factor priming-induced transendothelial migration of human eosinophils. *Allergy* 2015;70:805-12.
72. Meyer N, Akdis CA. Vascular endothelial growth factor as a key inducer of angiogenesis in the asthmatic airways. *Curr Allergy Asthma Rep* 2013;13:1-9.
73. Wang C, Zhang C-J, Martin BN, Bulek K, Kang Z, Zhao J, et al. IL-17 induced NOTCH1 activation in oligodendrocyte progenitor cells enhances proliferation and inflammatory gene expression. *Nat Commun* 2017;8:15508.
74. Grandbarbe L, Bouissac J, Rand M, Hrabé de Angelis M, Artavanis-Tsakonas S, Mohier E. Delta-Notch signaling controls the generation of neurons/glia from neural stem cells in a stepwise process. *Development* 2003;130:1391-402.
75. Argaw AT, Gurfein BT, Zhang Y, Zameer A, John GR. VEGF-mediated disruption of endothelial CLN-5 promotes blood-brain barrier breakdown. *Proc Natl Acad Sci U S A* 2009;106:1977-82.
76. Dudek KA, Dion-Albert L, Lebel M, LeClair K, Labrecque S, Tuck E, et al. Molecular adaptations of the blood-brain barrier promote stress resilience vs. depression. *Proc Natl Acad Sci U S A* 2020;117:3326-36.
77. Steine IM, Zayats T, Stansberg C, Pallesen S, Mrdalj J, Håvik B, et al. Implication of NOTCH1 gene in susceptibility to anxiety and depression among sexual abuse victims. *Transl Psychiatry* 2016;6:e977.
78. Auld DS, Robitaille R. Glial cells and neurotransmission. *Neuron* 2003;40:389-400.
79. Romanos J, Benke D, Saab AS, Zeilhofer HU, Santello M. Differences in glutamate uptake between cortical regions impact neuronal NMDA receptor activation. *Commun Biol* 2019;2:127.
80. Rosenkranz MA, Dean DC, Bendlin BB, Jarjour NN, Esnault S, Zetterberg H, et al. Neuroimaging and biomarker evidence of neurodegeneration in asthma. *J Allergy Clin Immunol* 2022;149:589-98.e6.

81. Lewkowich I, Ahlbrand R, Johnson E, McAlees J, Nawreen N, Raman R, et al. Modulation of fear behavior and neuroimmune alterations in house dust mite exposed A/J mice, a model of severe asthma. *Brain Behav Immun* 2020;88:688-98.
82. van Heerden JH, Conesa A, Stein DJ, Montaner D, Russell V, Illing N. Parallel changes in gene expression in peripheral blood mononuclear cells and the brain after maternal separation in the mouse. *BMC Res Notes* 2009;2:195.
83. Gatta E, Saudagar V, Drnevich J, Forrest MP, Auta J, Clark LV, et al. Concordance of immune-related markers in lymphocytes and prefrontal cortex in schizophrenia. *Schizophr Bull Open* 2021;2:sgab002.
84. Iturria-Medina Y, Khan AF, Adewale Q, Shirazi AH. Alzheimer's Disease Neuroimaging Initiative. Blood and brain gene expression trajectories mirror neuropathology and clinical deterioration in neurodegeneration. *Brain* 2020;143:661-73.